

# Investigating radiation patterns and power spectra from spherically symmetric explosive sources

CREWES Tech Talk  
Christopher Petten  
March 16<sup>th</sup>, 2012

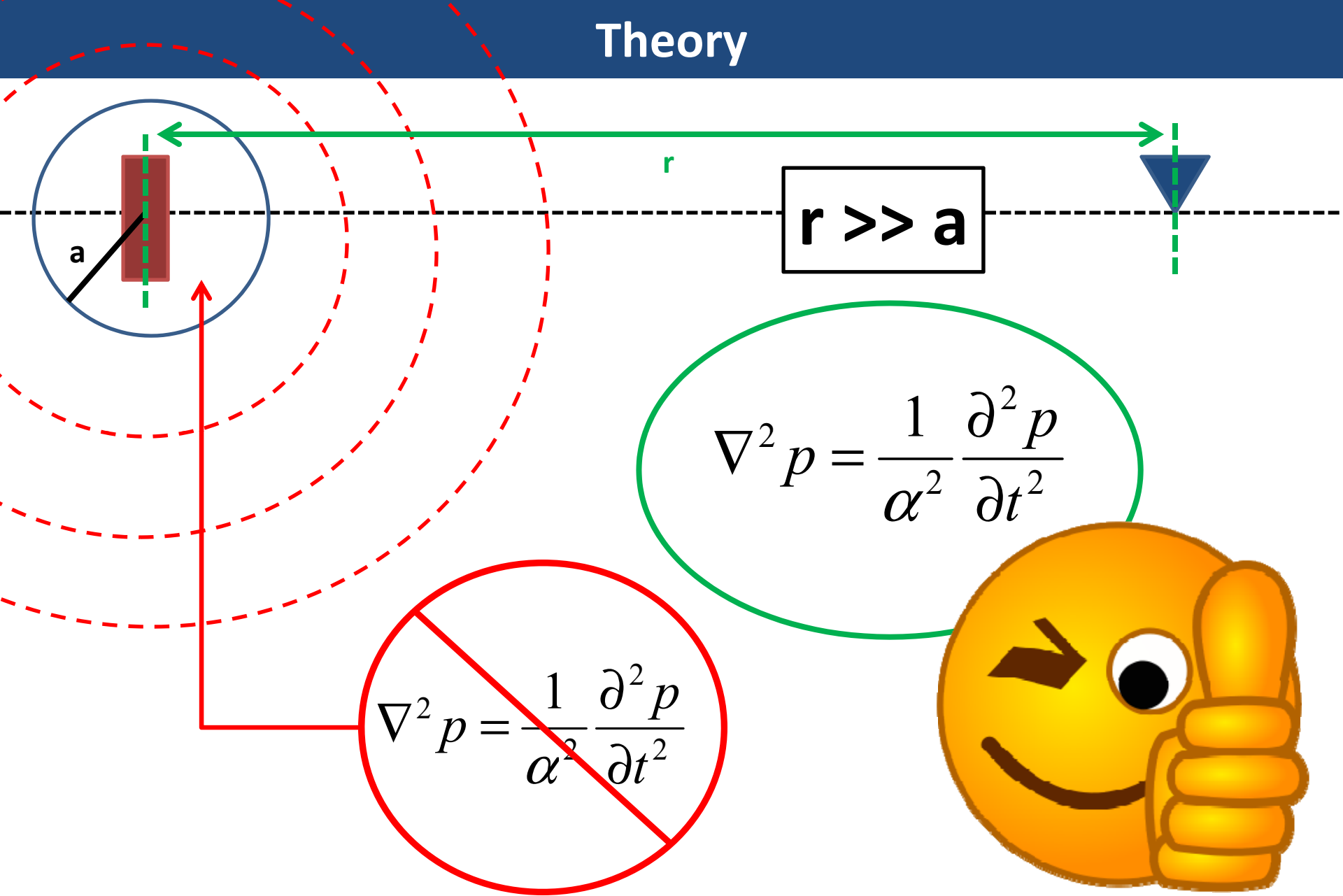
# Introduction

- ❖ Dynamite is a commonly used tool in exploration seismology to image the subsurface.
- ❖ The reflection component is of particular interest as it contains valuable information regarding the subsurface.
- ❖ Several models currently exist to theorize the radiation patterns emitted from a dynamite explosion.
- ❖ **We present the spherical model for dynamite and examine the effect of charge size on power and frequency spectra in a seismogram.**

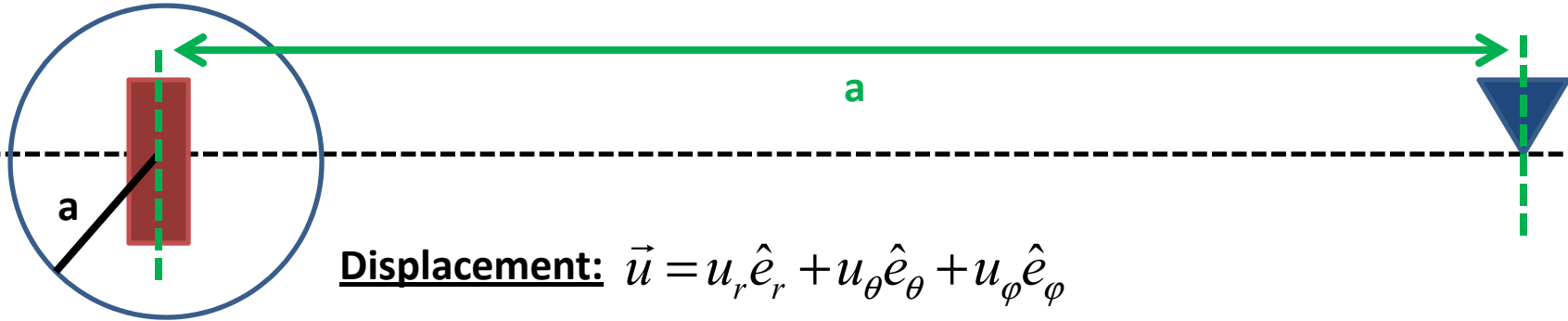


© Toons4Biz \* www.ClipartOf.com/6893

# Theory



# Displacement



**Displacement:**  $\vec{u} = u_r \hat{e}_r + u_\theta \hat{e}_\theta + u_\phi \hat{e}_\phi$

**Spherical Symmetry:**  $u_\theta = u_\phi = 0 \Rightarrow u = u_r$

$$u = \frac{\partial \phi}{\partial r} \rightarrow u_s(t_r) = \frac{a^2 p_o \sqrt{1-2\sigma}}{2\mu} \frac{e^{-ct_r}}{r} \sin(\chi t_r)$$

where

$$\chi = \frac{\alpha \sqrt{1-2\sigma}}{a(1-\sigma)} \quad c = \frac{\alpha}{a} \left( \frac{1-2\sigma}{1-\sigma} \right) \quad t_r = t - \frac{r-a}{\alpha}$$

# Observations

## Displacement

$$u_s(t_r) = \frac{a^2 p_o \sqrt{1-2\sigma}}{2\mu} \frac{e^{-ct_r}}{r} \sin(\chi t_r)$$

Frequency spectrum of u is:

$$f_o = \left[ \frac{\sqrt{1-2\sigma}}{2\pi(1-\sigma)} \right] \frac{\alpha}{a}$$

$$m \sim a$$

$$u \sim a$$

$$f \sim \frac{1}{a}$$

## Key Observations (Sharpe, 1942)

- ❖ Radius of the equivalent cavity,  $a$ , is proportional to the charge size.
- ❖ Particle displacement is proportional to the charge size.
- ❖ The dominant frequency of the emitted waves is inversely proportional to the charge size.
- ❖ The relationship between  $m$  and  $a$  is difficult to establish due to the nature of energy transfer when dynamite explodes.



# Data and Field Acquisition

- ❖ Data was obtained during the Hussar Low Frequency experiment conducted by CREWES in 2011.
- ❖ Groups of test charges, ranging in size between 1 and 4 kg, were buried at a depth of 15 m at 3 separate locations located along the seismic line (Margrave et al. 2011).
- ❖ Data was recorded by a 5-component geophone array; we used the vertical component of the 10 Hz receiver to conduct this study.
- ❖ The geophone and sample interval where  $\Delta x = 10$  m and  $\Delta t = 2$  ms.
- ❖ Data was collected for a total of 17 shots along the seismic line, however, this discussion will be limited to data from the first location.

# Power Analysis

- ❖ We were primarily interested in examining the power distribution in the first breaks, reflection data, and the ground roll.
- ❖ Each component of the seismogram was isolated using time windows represented by straight lines in x-t space.
- ❖ After each component was isolated, the power was computed by summing the squares of the traces contained within these windows.
- ❖ This procedure was carried out for all 17 shot records obtained from all the test charges.

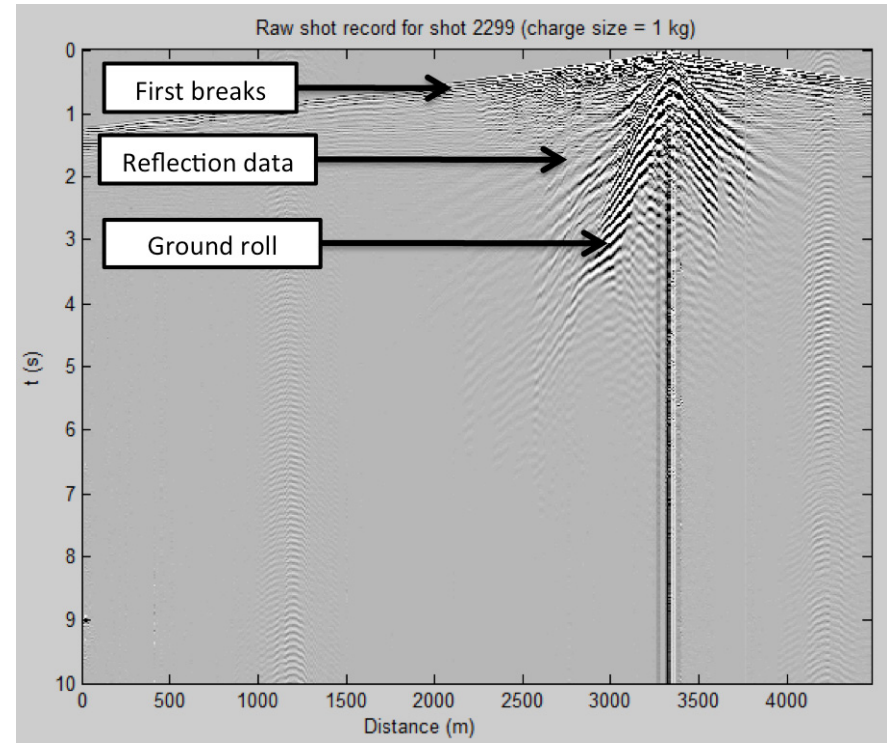
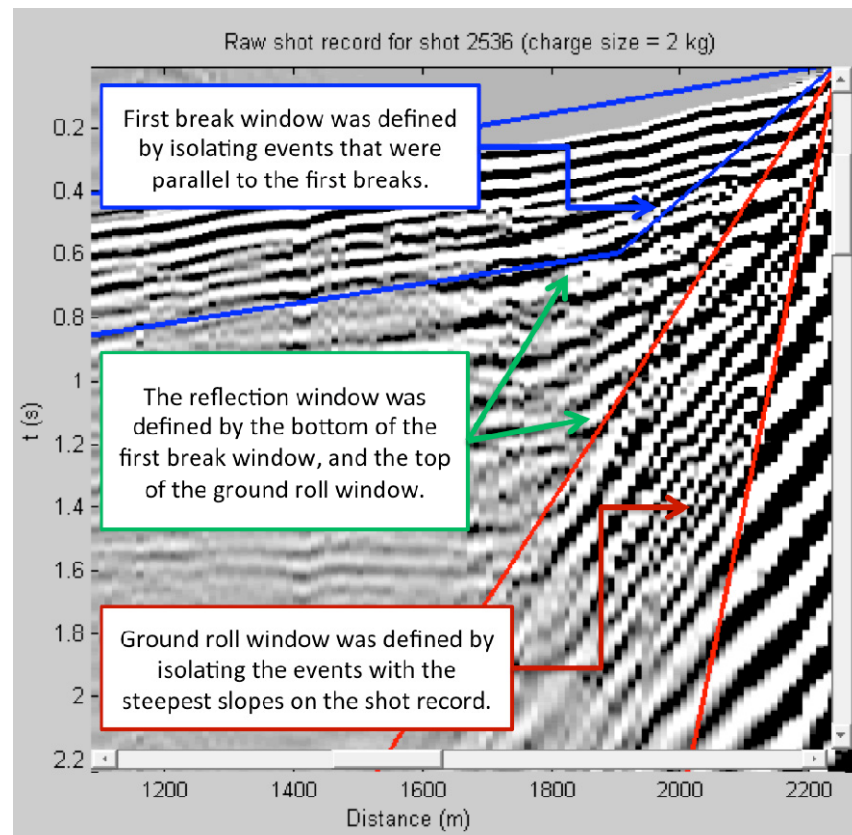
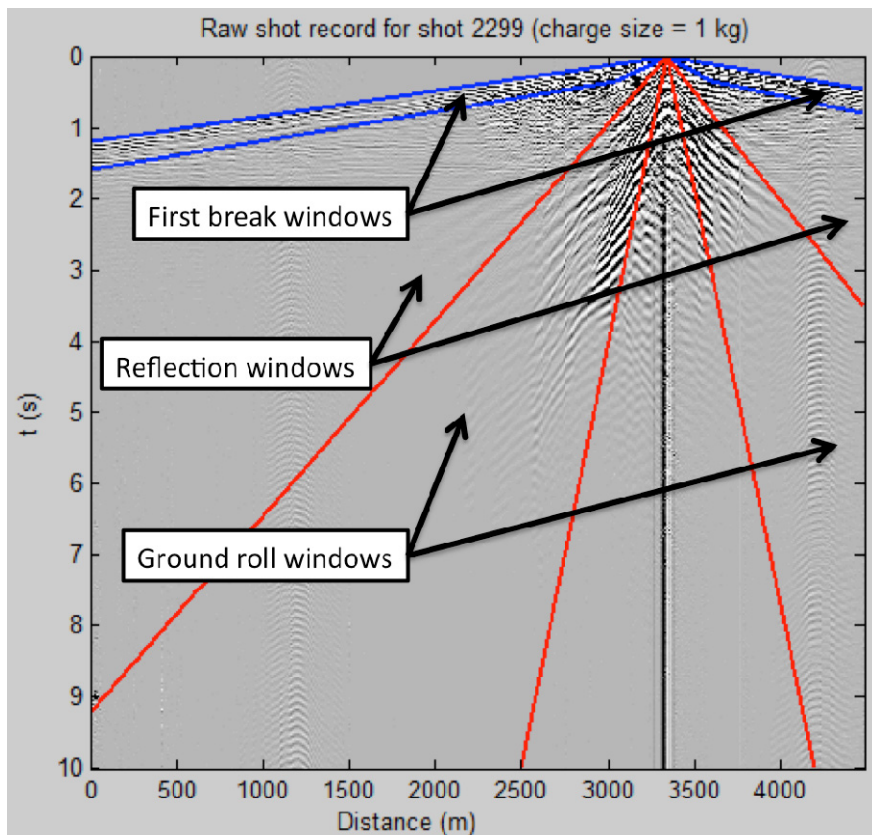


**FIG.1.** Raw shot record showing the individual components of the shot record that were analyzed in this investigation.

# Power Analysis



**(Left) FIG.2.** Raw shot record showing the time windows used to isolate each component of the shot record.

**(Right) FIG.3.** Criterion used to isolate the components from the remainder of the seismogram.

# Power Analysis

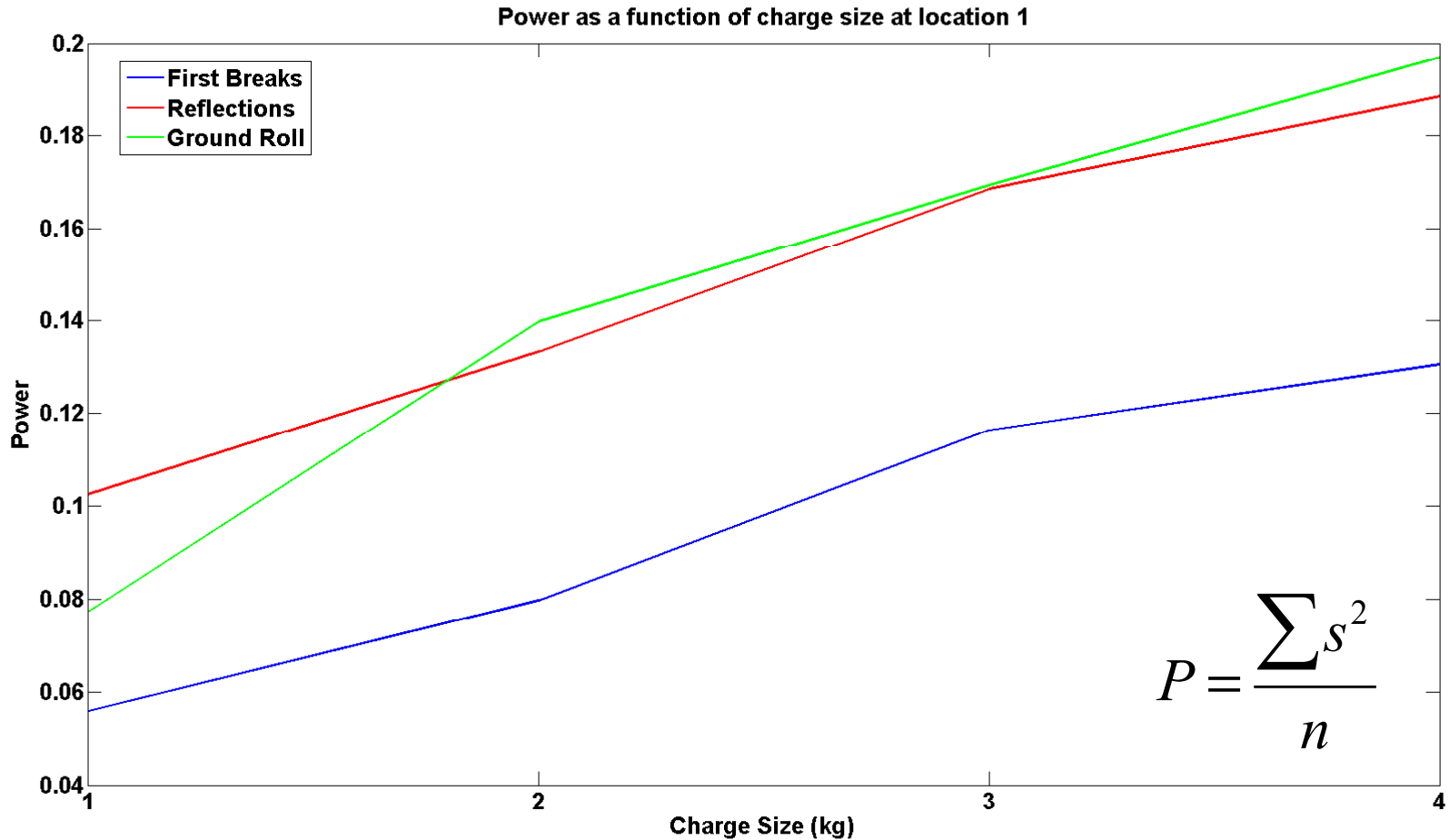


**FIG.3.** Shot power as a function of charge size at location one. The power, and thus displacement amplitude, appears to increase with charge size as predicted by Sharpe, 1942.

# Frequency Analysis

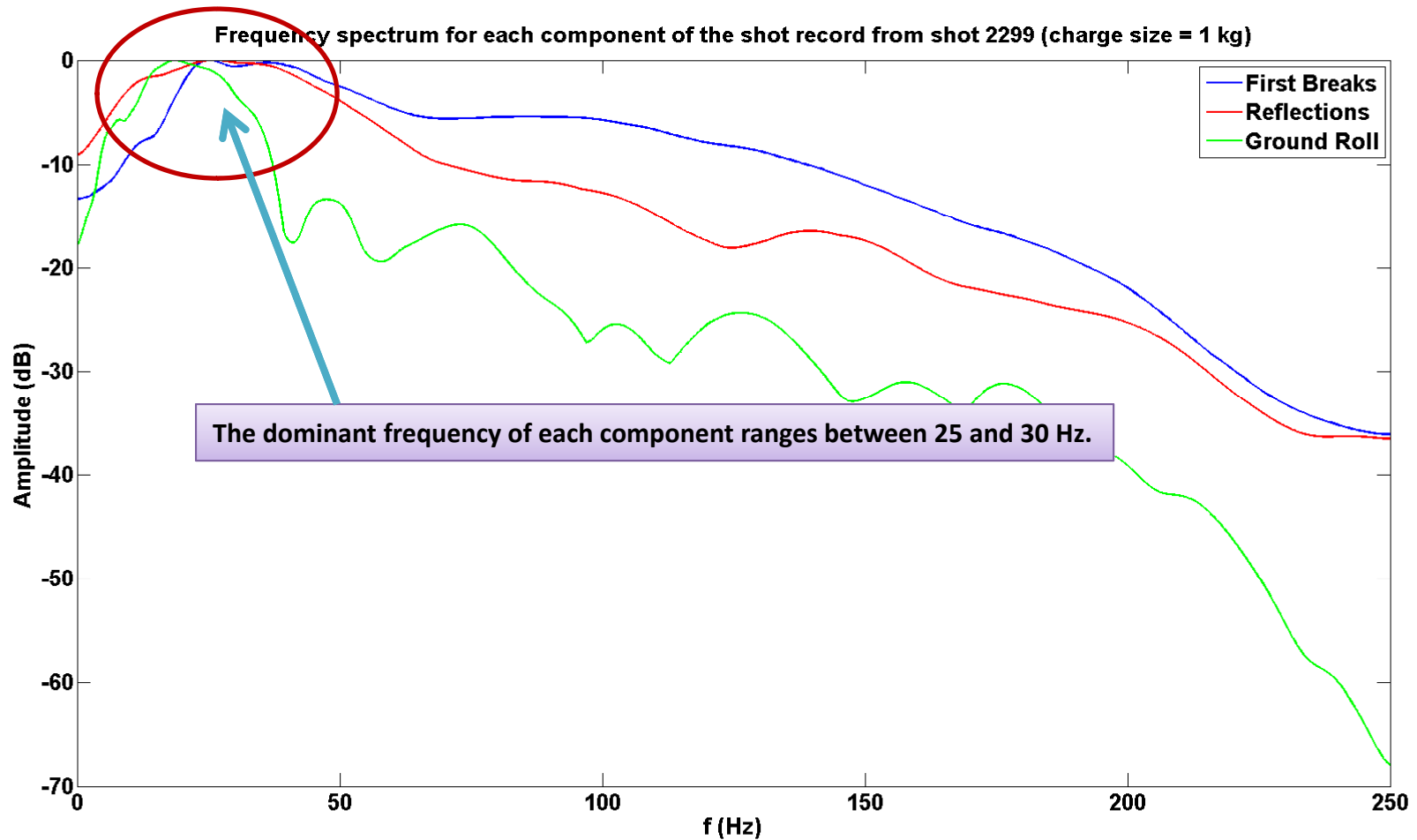


**FIG.4.** Frequency spectra for each of the components of the shot record for shot 2299. These were obtained via the `fxtran_new` code using the time windows for `tmin` and `tmax`.

# Frequency Analysis

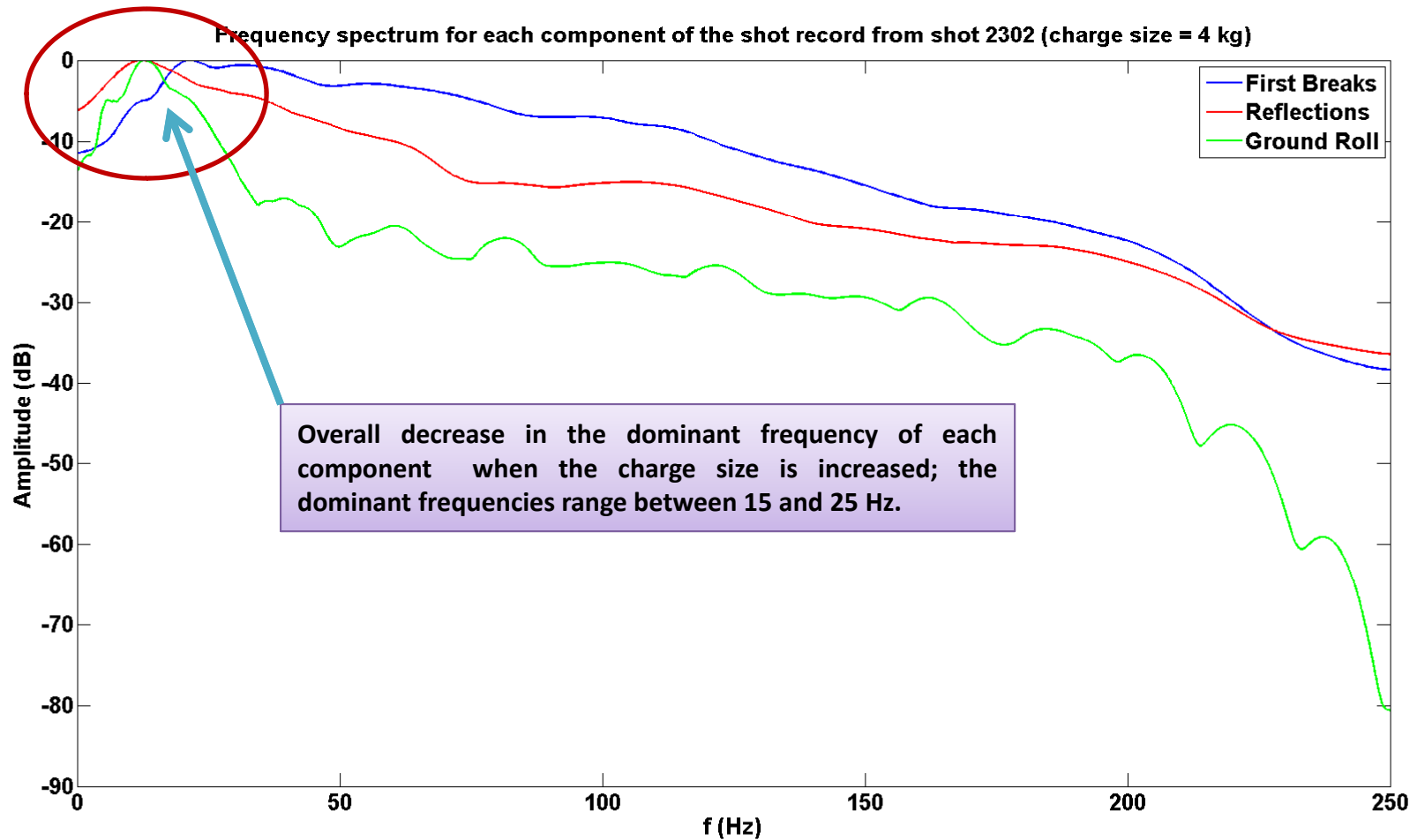


**FIG.5.** Frequency spectra for each of the components of the shot record for shot 2302. Note the decrease in frequency of each component with the increased charge size.

# Frequency Analysis

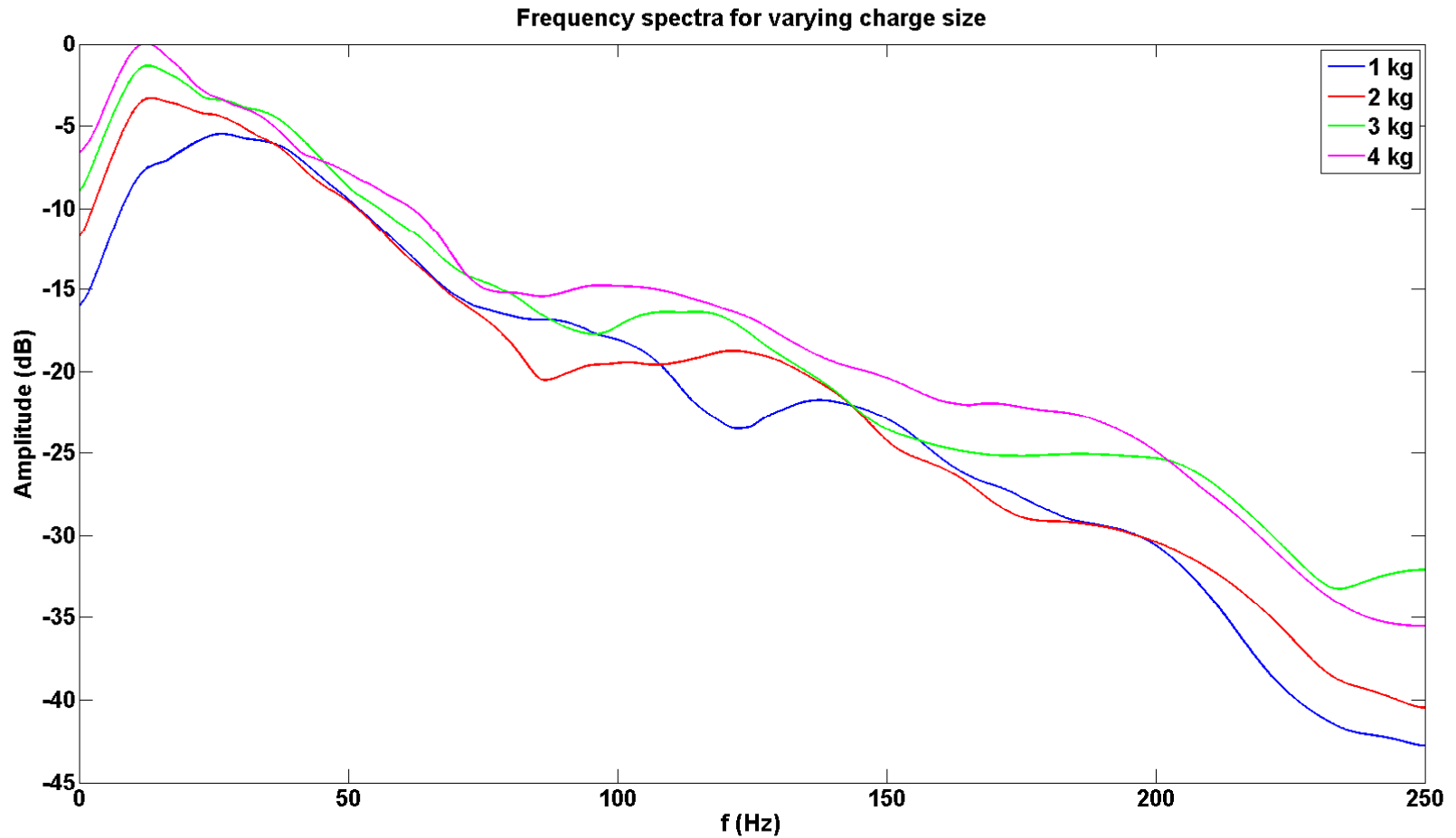


**FIG.6.** Frequency spectra for the reflections that result from different charge sizes. The dominant frequency appears to decrease with increased charge size as predicted by Sharpe, 1942.

# Frequency Analysis

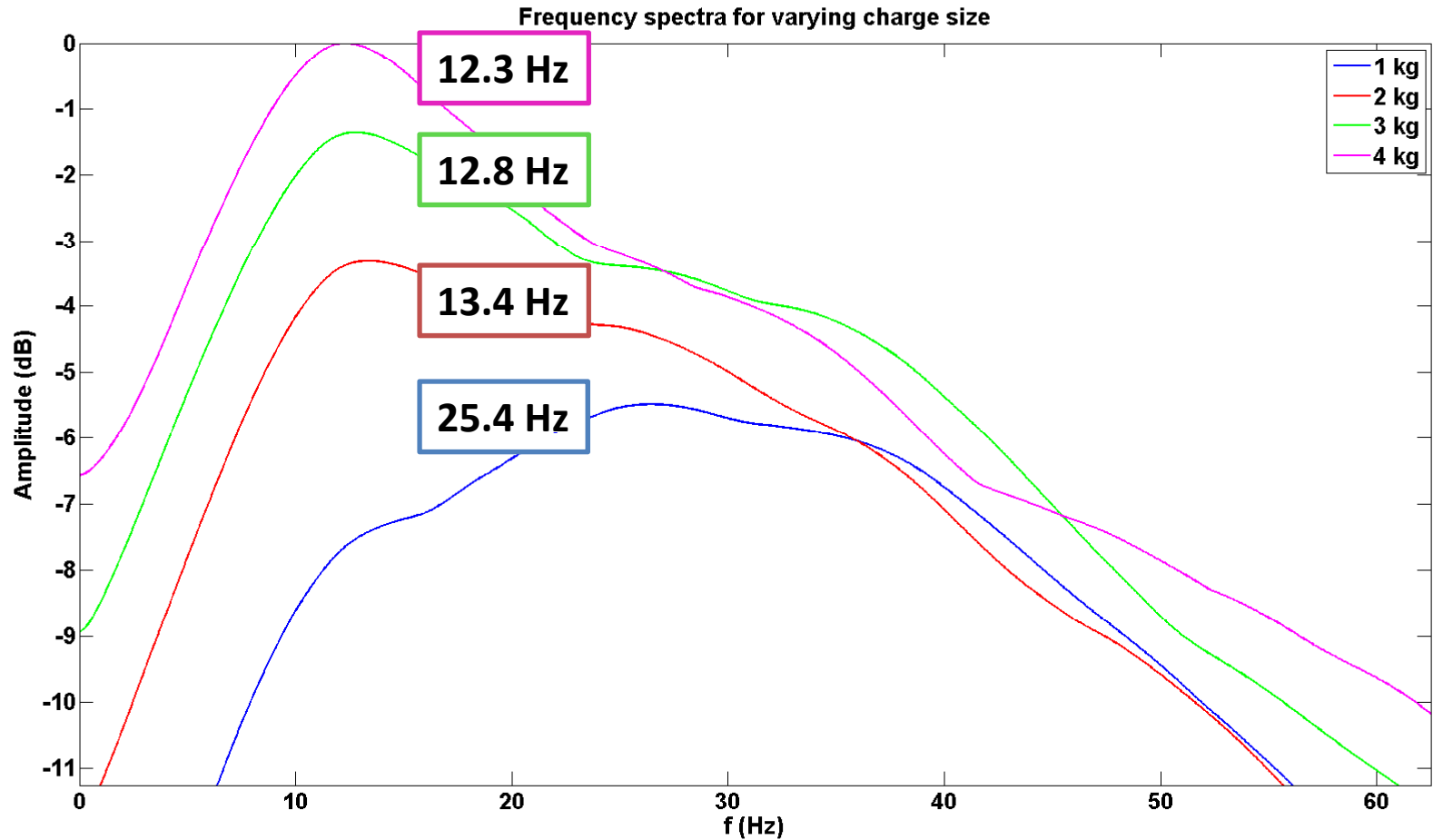


**FIG.7.** Closer view of the peaks in the frequency spectra for the reflection data. The decrease in frequency appears to be most drastic for the 1 and 2 kg charge sizes.

# Relationship between $m$ and $a$

Assume a relationship between dominant frequency and cavity size to be:

$$f_o = \lambda a^n$$

where:  $a \sim m$   
 $\lambda = \text{const.}$

Can we establish a relationship between cavity size and charge size? (we can't control  $a$ )

$$\log_{10} f_o = \log_{10} \lambda + n \log_{10} a$$

# Relationship between f and a

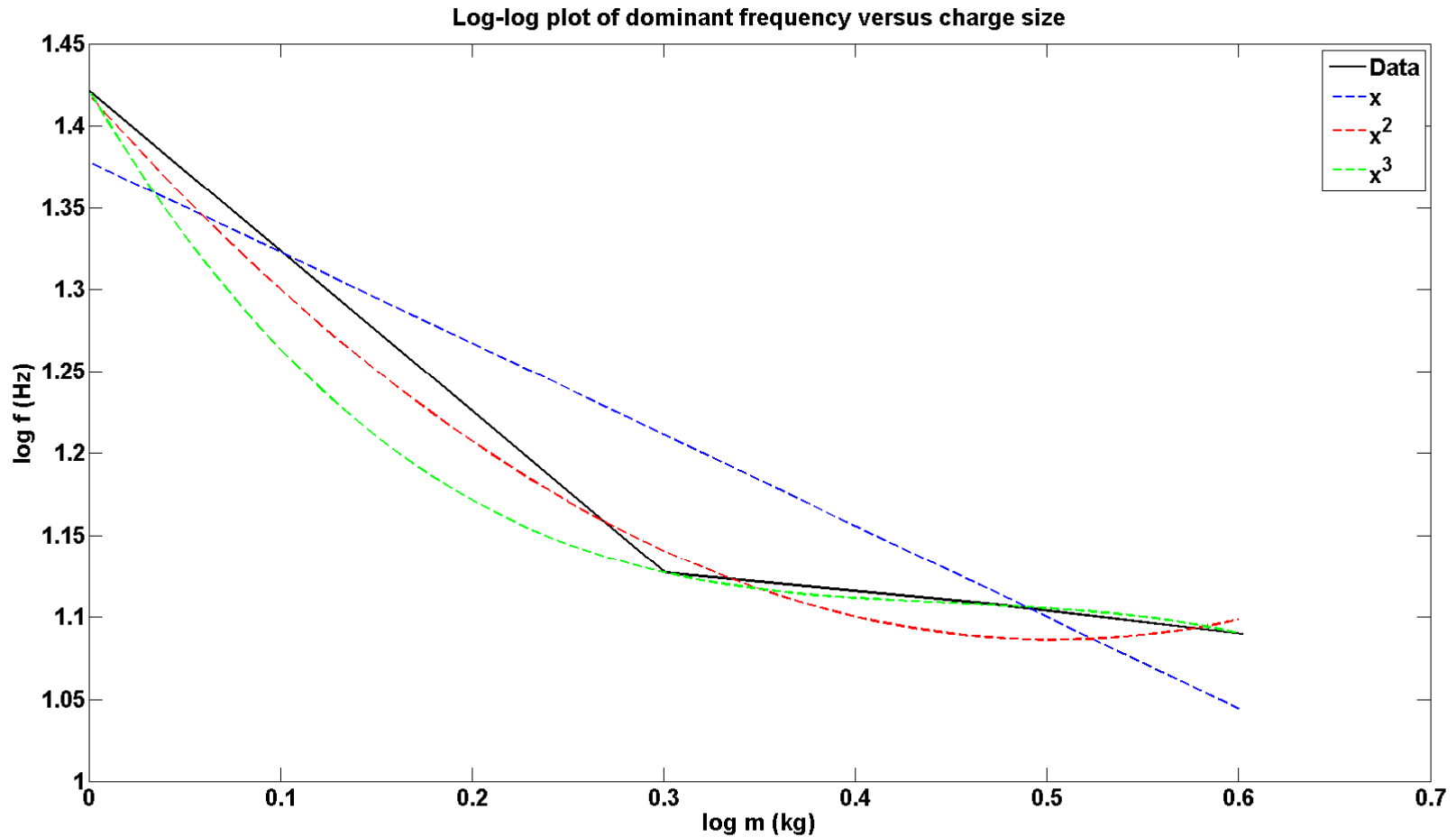


**FIG.8.** Log-log plot of dominant frequency and charge size. A series of polynomial fits which were computed based on the log of the charge size have been superimposed.

# Conclusions

- ❖ **The spherical model predicts that particle displacement increases with charge size.**
- ❖ **This model also predicts a decrease in dominant frequency with increased charge size.**
- ❖ **Increasing the size of the charge used will increase the power of reflection amplitudes.**
- ❖ **The dominant frequency of elastic waves emitted by a dynamite explosion decreases with charge size.**

# Acknowledgements

- ❖ I would like to thank Gary Margrave for his assistance with this project.
- ❖ All of the CREWES sponsors, staff, and students.